ELSEVIER

Thermochimica Acta 266 (1995) 373–384

thermochimica acta

The behavior of water molecules associated with structural changes in phosphatidylethanolamine assembly as studied by DSC ☆

Michiko Kodama *, Hidetaka Inoue, Yuji Tsuchida

Department of Biochemistry, Faculty of Science, Okayama University of Science, 1-1 Ridai-cho, Okayama 700, Japan

Abstract

The bilayer packing properties of dimyristoylphosphatidylethanolamine (DMPE), a hydrogen-bonding lipid, in aqueous medium were investigated from the thermal behavior associated with the lipid transition and ice-melting of frozen water. DMPE gel phase was obtained by cooling its liquid crystal phase converted into a stable crystal phase, most likely a three-dimensional crystal constituted of closely-stacked bilayers, by a specified two-step annealing treatment. On heating, the crystal phase transformed directly into the liquid crystal phase at 6 °C higher temperature (56.4 °C) and with a three times larger enthalpy (19.6 kcal mol^{-1}) than the gel-to-liquid-crystal phase transition. Estimation of the enthalpy change associated with the ice-melting peaks of the present system indicated that the conversion of the gel into crystal phases on annealing involves a change in water structure from a loosely-bound water (3 H_2O) to bulk free water caused by formation of lipid intermolecular hydrogen-bonding between adjacent bilayers.

Keywords: Crystal; DSC; Water

1. Introduction

The fundamental structure of biomembranes is a bilayer structure constituted of the major component, phospholipids. However, a great variety of phospholipids is present

* Corresponding author.

☆ Dedicated to Hiroshi Suga on the Occasion of his 65th Birthday.

SSDI 0040-6031(95)02449-2

in the membranes and a specific lipid composition occurs in different types of membranes [1]. This suggests that each of these membranes organizes a specific bilayer structure corresponding to its own function. Phosphatidylethanolamine (PE) is a widely occurring phospholipid in biomembranes, giving rise to dipolar zwitterions at neutral pH, similar to phosphatidylcholine (PC) which is the most abundant phospholipid in the membranes. Previous studies of PE have revealed that the adjacent lipids in the intrabilayer interact intermolecularly by hydrogen bonding between the amino (hydrogen-donating) and phosphate (hydrogen-accepting) groups [2–7] and this causes the gel-to-liquid-crystal phase transition to occur at a high temperature [4, 7, 8]. Presumably, the PE bilayer is stabilized by the intermolecular hydrogen bonding between the lipid head groups rather than with water molecules [9–11].

However, phase studies [4, 10–12] of the PE–water system have shown that two types of crystalline phases of different stabilities are present: the stable crystal phase transforms directly into the liquid crystal phase [12], in contrast to the less stable one which transforms into the liquid crystal phase by way of the gel phase [4]. In this connection, our previous studies [13, 14] of the PC–water system revealed that one type of crystalline phase present in this system incorporates a specific water which is intermediate between the so-called bound water and bulk free water. This water, characteristic of the crystal phase in the PC–water system, converted into bound water at the elevated temperature of the subtransition to the gel phase.

Based on these results, we investigated the PE–water system to clarify the different interactions of water molecules with the two lipids, PE and PC, depending on whether or not the hydrogen-donating group is incorporated in the molecule. The results obtained will be discussed with reference to the idea [7] that the intermolecular hydrogen-bonding between the lipid head groups involves the release of hydrogen-bonded water from the bilayer surface in such a way as indicated in Fig. 1. The thermotropic properties of PE and water molecules were studied by differential scanning calorimetry and structural information was obtained by negative-stain electron microscopy.

2. Experimental

2.1. Material

1,2-Dimyristoyl-*sn*-glycero-3-phophatidylethanolamine was purchased from Sigma and used without further purification. The lipid yielded a single spot by thin-layer chromatography on a silica gel plate using chloroform/methanol/7 M ammonia. Lipid concentrations were estimated by a modified Bartlett phosphate assay [15].

2.2. Sample preparations

DMPE samples for high-sensitivity differential scanning calorimetry were prepared as follows: the lipid film was first prepared by removing chloroform from the lipid stock solution on a rotary evaporator [16], and then under high vacuum (10^{-4} Pa) to

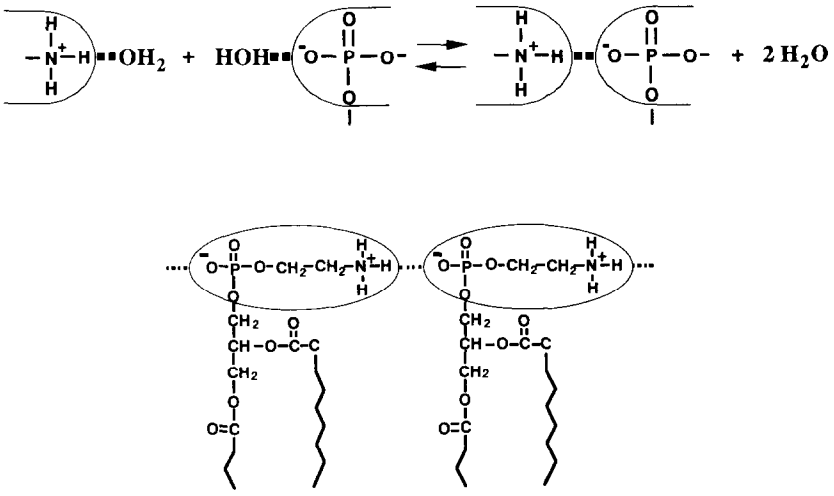

Fig. 1. Schematic illustration of PE intermolecular hydrogen bonding formation. The lipid intermolecular hydrogen bond is formed between the amino group of one molecule and the phosphate group of an adjacent molecule.

achieve complete removal of traces of the solvent. The dried lipid film was then suspended in distilled water, and gently vortexed at the liquid crystal temperature.

For low-temperature calorimetry, the dehydrated lipid film was prepared in the high-pressure crucible cell of a Mettler apparatus according to the above-described method and then sealed off in a dry box filled with dry N_2 gas to determine the weight of the lipid. Increasing amounts of water were added stepwise to the lipid film using a microsyringe to prepare DMPE samples of different, rather low water contents up to approx. 33 g% of water. All samples were annealed by repeated thermal cycling at temperatures above and below the T_M transition to ensure homogeneous mixing and to attain the equilibrium state.

2.3. *Differential scanning calorimetry*

Calorimetric experiments were performed with two types of differential scanning calorimeters, a Microcal MC2 and a Mettler TA-4000, both operated under computer control for automatic data collection and analysis. Scanning rates of 45° and 60°C h^{-1} on heating were used for the Microcal and Mettler calorimeters, respectively, unless otherwise specified.

2.4. *Electron microscopy*

Negative-stain electron microscopic experiments with sodium phospho-tungstate (pH approx. 7) [17] were performed with a JEOL JEM-2000EX electron microscope operated at 200 kV at around 20°C. Sample preparations for this experiment were carried out according to the procedure previously employed by us [18].

3. Results

3.1. Thermal behavior of DMPE in excess water

Fig. 2 shows typical thermotropic behavior of the DMPE–water system at a lipid concentration of 2 mM (99.9 g% of water) obtained by high-sensitivity differential scanning calorimetry (Microcal MC2). Fig. 3 gives a schematic diagram of relative enthalpy (H) versus temperature (t) curves constructed on the basis of the enthalpy changes and transition temperatures associated with the phase transitions shown in Fig. 2. By reference to Fig. 2 and following the three curves of H vs. t shown in Fig. 3, the phase behavior of the present system can be explained as follows: the gel phase obtained by cooling the liquid crystal phase is transformed into the liquid crystal phase at the T_M transition (50.2 °C) on heating (see curve (a) of Fig. 2), but is allowed to persist as a metastable state, even at a temperature as low as −50 °C, on cooling. However, if the gel phase sample is annealed under specified conditions, it converts into either of two crystalline phases with different stabilities depending upon the annealing treatment adopted. That is, the conversion into a less stable crystalline phase occurs when the gel sample is stored at around −5 °C for at least five days and this crystal phase transforms into the gel phase at the temperature of the T_L transition (43.4 °C),

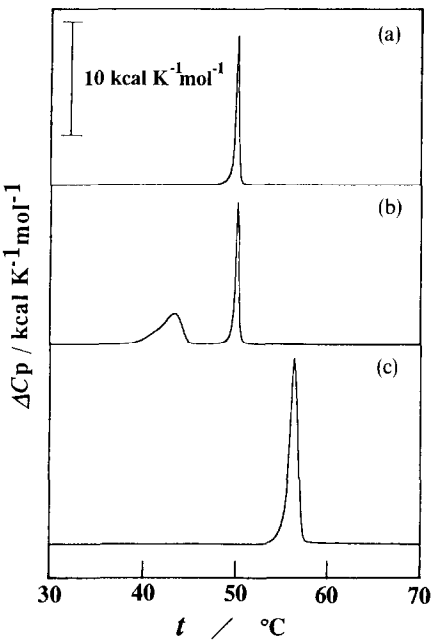

Fig. 2. Typical phase transition behavior in the DMPE–water system. The apparent, excess heat capacity (ΔC_p) is plotted as a function of temperature (t). The three curves (a), (b) and (c) are characterized by the phase transitions T_M (gel to liquid-crystal), T_L (less stable crystal to gel) followed successively by T_M, and T_H (stable crystal to liquid-crystal), respectively.

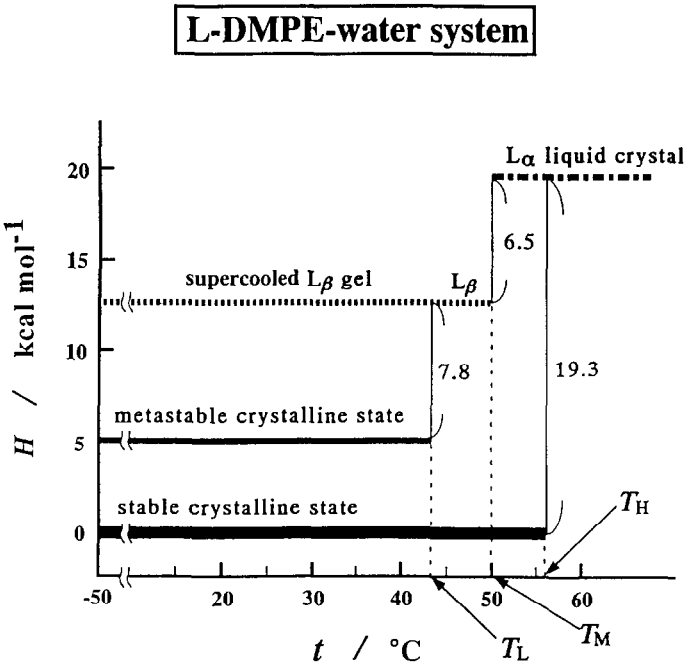

Fig. 3. Schematic diagram of relative enthalpy (H) versus temperature (t) curves in the DMPE–water system. In this diagram, enthalpy curves of the gel and metastable crystal phases relative to that of the stable crystal phase taken as zero value are compared.

successively followed by the T_M transition (see curve (b) of Fig. 2). When the alternative two-step annealing (detailed below) is applied to the gel sample, it causes the gel to convert into a stable crystal phase which shows a direct transition (T_H) to the liquid crystal phase at about 6 °C higher temperature and with a three times larger enthalpy than the gel-to-liquid crystal phase transition (see curve (c) of Fig. 2). The high-temperature transition, T_H, characteristic of the stable crystal phase, is no longer realized in a repeated heating scan after cooling the liquid crystal phase and is replaced by the T_M transition.

To clarify the essential difference between the T_M and T_H transitions to the liquid crystal phase, we investigated, in detail, the lipid–lipid and/or lipid–water interactions in the gel and stable crystal phases.

3.2. *Conversion of gel into stable crystal phases on annealing*

Fig. 4 shows a negative-stain electron micrograph of the DMPE gel phase. In this electron micrograph, the lipid bilayers (white regions) and water layers (black regions) are alternately arranged. In addition, although the gel phase sample was prepared according to the Bangham method for the preparation of vesicles, the surface of the bilayers shown in Fig. 4 is planar, not the generally accepted curved surface for

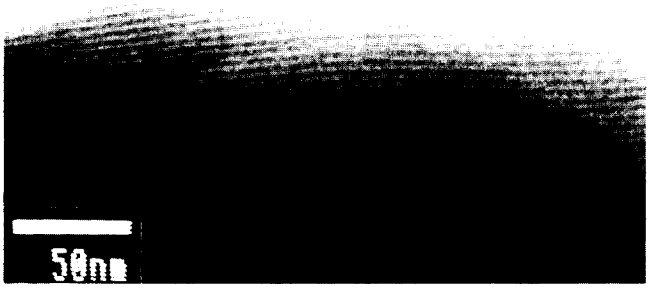

Fig. 4. Negative-stain electron micrograph of DMPE gel-phase sample prepared according to the Bangham method.

a vesicular structure [18]. The planar surface suggests that the PE head groups are closely packed on the bilayer surface. This seems to be concerned with the fact that PE has an intermolecular hydrogen-bond-forming property and the lipid head group occupies a small cross-sectional area [2, 3].

However, complete conversion of the gel to a stable crystalline phase was attained by two-step annealing at different temperatures. That is, the primary process, i.e. nucleation of the crystalline phase, requires the gel phase sample to be heated from -50 to $-10\,^{\circ}C$ at a scanning rate as slow as $0.1\,^{\circ}C\ min^{-1}$. Subsequent heating at the same scanning rate causes an exothermic peak due to nuclear growth in place of the endothermic T_M transition peak and this exothermic peak is immediately followed by an incomplete, endothermic peak due to the partial crystal-to-liquid-crystal phase transition, as shown in curve (b) of Fig. 5. In contrast, for the sample which has not experienced the primary process, no peak other than the T_M transition peak is observed on heating at the slow scanning rate of $0.1\,^{\circ}C\ min^{-1}$, as shown in curve (a) of Fig. 5. Based on these facts, the second process for nuclear growth after the nucleation process is confirmed to be an incubation at around 47–48 °C (exothermic temperature). The sample subjected to the above-described two-step annealing shows the well-developed endothermic peak of the T_H transition shown in curve (c) of Fig. 2. The stable crystalline phase in the electron micrograph is most likely a three-dimensional crystal consisting of closely stacked bilayers, showing a lack of interbilayer water, in contrast with the gel phase.

3.3. *Thermal behavior of water molecules in the gel and stable crystal phases*

The water structures in the gel and stable crystal phases were investigated from the melting behavior of frozen water. In Fig. 6, a series of ice melting and lipid transition peaks (T_M and T_H) are compared between the gel (A) and stable crystal phases (B) at different water contents. Above approx. 21 g% water, the limiting peaks of both the T_M and T_H transitions are observed. Sharp ice-melting peaks at around 0 °C are observed

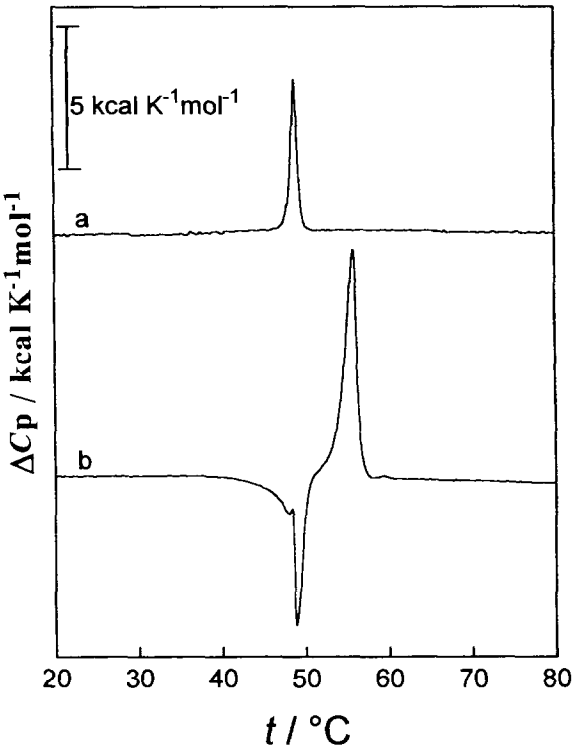

Fig. 5. Effect of the annealing treatment on the thermal behavior associated with the T_H transition for DMPE sample containing 29.9 g% water.

for all the gel and crystal phases at different water contents represented in this figure. However, when the sharp ice-melting peaks at 0 °C are compared between both phases at the same water content, a larger area is seen for the crystal phase than that for the gel phase at all water contents. This difference is clearly recognized by the enlarged ice-melting curves shown in Fig. 7. In this figure, two curves at lower water contents are added. As is obvious from Fig. 7(A), the gel phase is characterized by a broad ice-melting peak starting from approx. − 30 °C, successively followed by the sharp peak at around 0 °C. Furthermore, the limiting, broad ice-melting peak is observed at water contents higher than 14.4 g%. Fig. 8 shows the result of deconvolution analysis of the ice-melting curve for the gel phase at 14.4 g% water as an example: the ice-melting peak is composed of three components indicating two components of the broad ice-melting peak at midpoint temperatures of −17 and −6 °C, respectively. In contrast, for the crystal phases shown in Fig. 7(B), no ice-melting peak other than the sharp peak at around 0 °C is observed, regardless of water content. This fact indicates that the larger area of the sharp peak observed for the crystal phase compared with the gel phase is caused by a transformation of the broad peak into its sharp peak, which is involved in the conversion of the gel into liquid crystal phases on annealing.

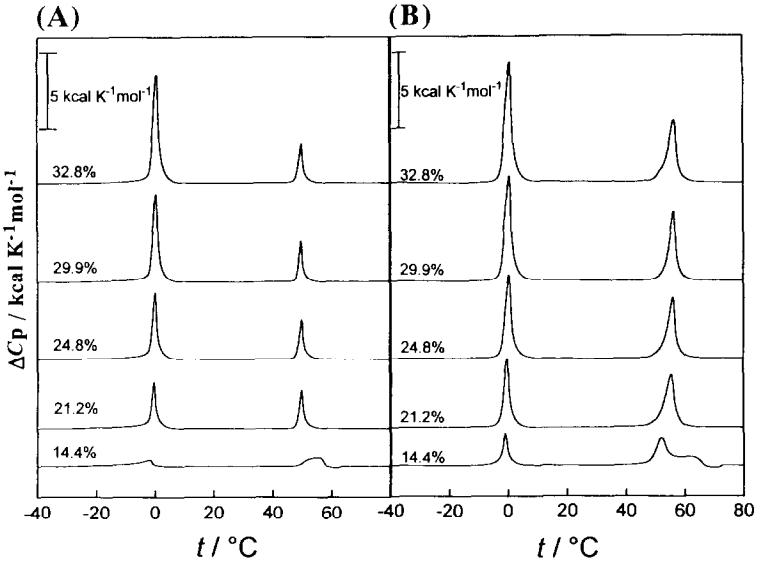

Fig. 6. Comparison between the thermal behavior of gel (A) and stable crystal (B) phase samples of increasing water content (g%) on heating from −50 to 80 °C. The transitions of the gel and crystal phases to liquid-crystal phase are characterized by the T_M and T_H transition peaks, respectively.

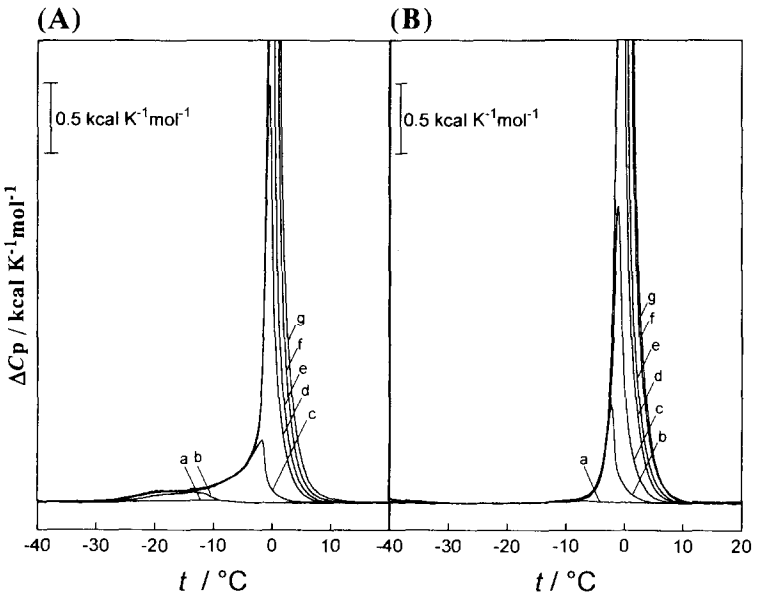

Fig. 7. Comparison of enlarged ice-melting curves for gel (A) and stable crystal (B) phase samples of increasing water content. Water content (g%): (a) 2.3; (b) 8.4; (c) 14.4; (d) 21.2; (e) 24.8; (f) 29.9; (g) 32.8.

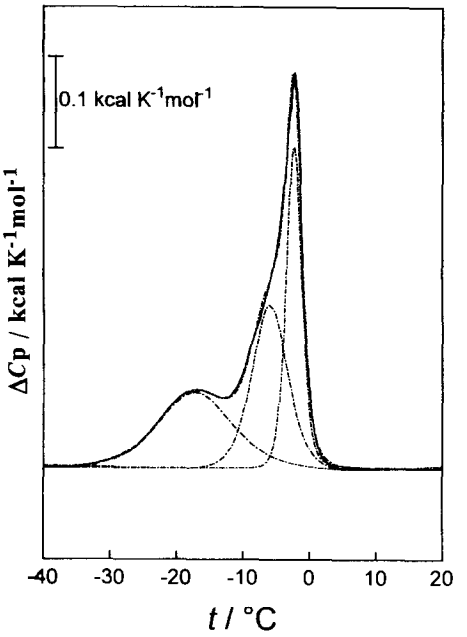

Fig. 8. Deconvolution analysis of ice-melting curve for gel phase sample containing 14.4 g% water. The deconvolution was performed on the basis of a computer program attached to a Microcal calorimeter [18]. Three deconvolved curves as well as a theoretical curve are shown by the dotted lines. The apparent, excess heat capacity (ΔC_p) is plotted as a function of temperature (t).

To elucidate quantitatively the difference in water structure between the gel and crystal phases, the enthalpy changes (ΔH) associated with the sharp ice-melting peaks were compared between both phases at various water contents. For the gel phase, the enthalpy change was estimated from the deconvolved curve of the sharp component at around 0 °C shown in Fig. 8 as an example. The results are shown in Fig. 9, where the enthalpy change is plotted against the mole numbers of water added to a mole of DMPE. In this figure, the bold line indicates the theoretical curve obtained from the melting enthalpy of hexagonal ice, on the assumption that all the water added to the sample is present as free water. As shown in Fig. 9, parallel to the theoretical curve, the ΔH curves for both the crystal and gel phases increase, starting at 1 H_2O (2.9 g% water) and 4 H_2O (10.0 g% water), respectively. Comparison of the three curves (theoretical, crystal and gel) shown in Fig. 9 gives the following results:

(a) The difference in ΔH of the theoretical and crystal curves at the same water content corresponds to the amount of water which does not crystallize on cooling to −50 °C. This non-freezable water present in the gel phase is considered to exist as interlamellar water tightly bound to the lipid head groups and reaches a maximum at 1 H_2O per mole of DMPE. Beyond this content, all the water added exists as bulk free water (the sharp component of the ice-melting peak) and coexists with the crystal phase.

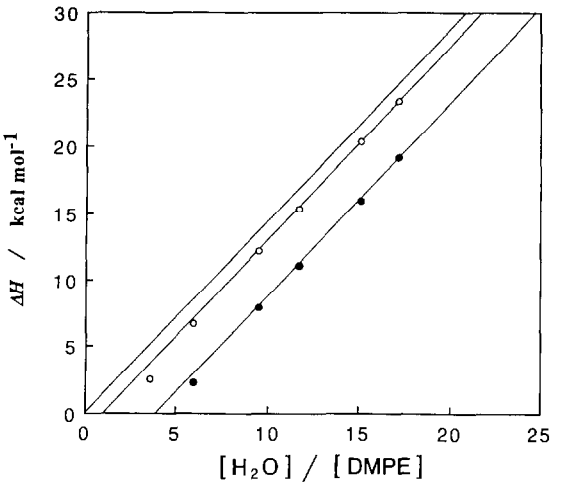

Fig. 9. Comparison of the enthalpy changes (ΔH) associated with the sharp ice-melting peaks at around 0 °C for gel (●) and stable crystal (○) phase samples at various water contents. The enthalpy change is plotted against mole numbers of water added to a mole of DMPE. The bold line shows a theoretical curve obtained from the melting enthalpy of hexagonal ice.

This result accounts well for the absence of a peak due to ice melting observed for a sample of 2.3 g% water (see curve (a) of Fig. 7(B)).

(b) The difference between ΔH of the crystal and gel curves at the same water content corresponds to the amount of water which is loosely bound to the lipid head groups (the broad component of the ice-melting peak) in the gel phase, but exists as bulk free water in the crystal phase. This phenomenon is clearly seen in a sample of 8.4 g% water (see curves (b) of Fig. 7(A) and (B)). The limiting, maximum uptake of this bound water into the gel phase is shown to be 3 H_2O. Therefore, the interlamellar water of the gel phase is composed of 3 H_2O loosely bound water and 1 H_2O non-freezable, tightly bound water.

4. Discussion

The X-ray crystallographic study of dilauryl-DLPE grown from acetic acid has shown that adjacent bilayers of DLPE are linked via a hydrogen bond arrangement involving the acetic acid molecules [2, 3, 7]. Such a hydrogen-bond linkage could be formed when the acetic acid is replaced by a water molecule. Thus, the tightly bound water (1 H_2O) of the stable crystal phase discovered here is presumed to form hydrogen bonds with each of the opposite lipid head groups in adjacent bilayers [6], resulting in the closely stacked bilayer crystal in the present DMPE–water system. In this sense, the tightly bound water of the crystal phase is apparently distinguished from that of the gel phase.

However, in the present system, the loosely bound water (3 H_2O), characteristic of the gel phase is released outside the bilayers as the bulk free water if the specified

annealing is adopted. Such a drastic change in water structure involved in the conversion of the gel into crystal phases is not observed for the PC–water system previously investigated by us [13, 14]. That is, on annealing the loosely bound water of the PC gel-phase changes into a more loosely bound water and remains as interlamellar water of the crystal phase. Taking into account that the transition mode of the PE crystal phase is different from that of the PC crystal which transforms into the liquid crystal phase by way of the gel phase, the following results can be given for the present system: as any interlamellar water other than the tightly bound water is not incorporated into the PE crystal phase, the crystal phase is unable to transform into the gel phase which results from the increased interaction between lipid and water molecules [19–21]. The interlameller water necessary for appearance of the gel phase is interposed, for the first time, between the bilayers at the elevated temperature of the T_H transition to the liquid crystal phase of a liquid-like state, so that the direct transition of PE crystal to the liquid crystal phase occurs and the PE phase is realized only by cooling the liquid crystal phase.

Furthermore, the above-described results suggest that in the present crystal phase, adjacent bilayers interact strongly by attractive forces other than their hydrogen bonds with the tightly bound water. Considering PE as the intermolecular hydrogen-bonding lipid, interbilayer hydrogen bonding is suggested as another attractive interbilayer force [6, 7] and this hydrogen bonding is considered to be formed between the lipids opposite to each other in the interbilayer in a way such as shown in Fig. 1. Accordingly, it is stated that the interbilayer hydrogen-bonding formation is a dominant process in the conversion of the gel into crystal phases on annealing. Furthermore, focusing on the role of water molecules in this hydrogen bonding formation by reference to Fig. 1, it is seen that the extra, bulk free water observed for the stable crystal phase results from a release of the hydrogen-bonded water (loosely bound water in the gel phase) from amino and phosphate groups caused by each group participating in the interbilayer hydrogen bonding.

References

[1] R. Harrison and G.G. Lunt, Biological Membranes, 2nd edn., Blackie and Son Ltd., London, 1980, p. 68.
[2] M. Elder, P. Hitchcock, R. Mason and G.G. Shipley, Proc. R. Soc. London Ser. A, 354 (1977) 157.
[3] G.G. Shipley, in D.M. Small (Ed.), Handbook of Lipid Research, Vol. 4, Plenum Press, New York, 1986, p. 97.
[4] S. Mulukutla and G.G. Shipley, Biochemistry, 23 (1984) 2514.
[5] H. Akutsu, M. Ikematsu and Y. Kyogoku, Chem. Phys. Lipids, 28 (1981) 149.
[6] T.J. McIntosh and S.A. Simon, Biochemistry, 25 (1986) 4948.
[7] J.M. Boggs, Biochim. Biophys. Acta, 906 (1987) 353.
[8] J.F. Nagle, J. Membrane Biol., 27 (1976) 233.
[9] H.H. Mantsch, S.C. Hsi, K.W. Butler and D.G. Cameron, Biochim. Biophys. Acta, 728 (1983) 325.
[10] J. Silvius, P.M. Brown and T.J. O'Leary, Biochemistry, 25 (1986) 4249.
[11] P.M. Brown, J. Steers, S.W. Hui, P.L. Yeagle and J.R. Silvius, Biochemistry, 25 (1986) 4259.
[12] D.A. Wilkinson and J.F. Nagle, Biochemistry, 23 (1984) 1538.
[13] M. Kodama, Thermochim. Acta, 109 (1986) 81.

[14] M. Kodama, Y. Hashigami and S. Seki, J. Colloid Interface Sci., 117 (1987) 497.
[15] G.V. Marinetti, J. Lipid Res., 3 (1962) 1.
[16] A.D. Bangham, M.W. Hill and N.G. Miller, Methods Membr. Biol., 1 (1974) 1.
[17] S.E. Schullery, C.F. Schmidt, P. Felgner, T.W. Tillack and T.E. Thompson, Biochemistry, 19 (1980) 3919.
[18] M. Kodama, T. Miyata and Y. Takaichi, Biochim. Biophys. Acta, 1169 (1993) 90.
[19] M. Kodama, K. Tsujii and S. Seki, J. Phys. Chem., 94 (1990) 815.
[20] M. Kodama and S. Seki, J. Colloid Interface Sci., 117 (1987) 485.
[21] M. Kodama and S. Seki, Adv. Colloid Interface Sci., 35 (1991) 1.